

## Synthesis, Characterization and Adsorption Capability of CdO Microstructure for Congo Red from Aqueous Solution

A. Tadjarodi<sup>a\*</sup>, H. Kerdari<sup>b</sup>, M. Imani<sup>a</sup>

<sup>a</sup>Research Laboratory of Inorganic Materials Synthesis, Department of Chemistry, Iran University of Science and Technology, 16846-13114, Tehran, Iran

<sup>b</sup>Department of Chemistry, Saveh Branch, Islamic Azad University, Saveh, Iran

### Article history:

Received 13/1/2012

Accepted 20/5/2012

Published online 1/6/2012

### Keywords:

Nanostructures

Semiconductor

Adsorption

Cadmium oxide

Congo Red

### \*Corresponding author:

E-mail address:

[tajarodi@iust.ac.ir](mailto:tajarodi@iust.ac.ir)

Phone: +98 (21) 77240516

Fax: +98 (21) 77491204

### Abstract

Cadmium oxide rhombus-shaped nanostructure was synthesized using hydrothermal process followed by heating treatment. Clearly, X-ray diffraction pattern demonstrated the formation of CdO crystalline phase. Scanning electron microscopy (SEM) showed that the obtained rhombus-like structure is composed of nanoparticles with the average size of 29 nm. In addition, we evaluated adsorption of organic dye i.e. Congo red from water using the prepared CdO rhombus like microstructure. UV-visible absorption spectroscopy was used to record the adsorption behavior. It was found that the removal process is performed via electrostatic absorption mechanism. The maximum adsorption capacity of CdO rhombus structures (0.01 g) for Congo Red (CR) in the concentration range (5-50 mg L<sup>-1</sup>) studied, as calculated from the Langmuir isotherm model at 25 °C and neutral pH, was found to be 41.20 mg g<sup>-1</sup>.

2012 JNS All rights reserved

## 1. Introduction

Nowadays, due to optical and electrical properties, semiconductor metal oxides in nanoscale have been nominated for various applications in several scientific and industrial fields. Cadmium oxide, CdO, is a known n-type semiconductor with the direct band gap energy of 2.2-2.5 eV and the indirect band gap of 1.36-1.98

eV [1-4]. In fact, the lattice's defects in the crystalline structure are led to difference at the band gap energy [5]. This material is synthesized by numerous methods such as microemulsion [2], chemical vapour deposition [5], sol-gel process [6, 7], sonochemical technique [8], hydrothermal/solvothermal method [9-11] and mechanochemical process [12, 13]. Hydrothermal

reaction can be a beneficial technique to prepare various nanostructures amongst methods so that more researchers prefer it to others [14].

CdO has not only the unique optical and optoelectrical characteristics but also has the selective catalytic properties that can be used to photodegrade some of the organic compounds, dyes, pigments and many of environmental pollutants [15-17].

In various industries such as textile, food, paper and dyeing industries, different pigments and dyes are used to color products. The use of these colored compounds produces colored wastewaters, which lead to environmental pollutions. These pollutants have to be eliminated before discharging into environment. Congo red (CR) is the anionic hazardous organic dye, which despite being banned, it is still widely consumed in several industries. Many techniques such as electrochemical, sonochemical, photocatalytic oxidation and adsorption methods have been employed to remove these pollutions from water bodies and refinement of wastewater. Adsorption is a suitable, low-cost, available treatment for this aim [18-21]. In this research, the rhombus-shaped structures of cadmium oxide consisting of the nanoparticles were synthesized by hydrothermal process followed by calcination treatment. In the next stage, the obtained product was employed for removing CR by adsorption removal at room temperature and natural pH. To the best of our knowledge, decontamination of CR dye by CdO rhombus particles has not been reported yet.

The resultant products were characterized by using FT-IR, XRD, TGA and SEM techniques.

## 2 Experimental

### 2.1. Materials

Cadmium chloride monohydrate ( $\text{CdCl}_2 \cdot \text{H}_2\text{O}$ , Merck, pure), ammonium oxalate monohydrate ( $(\text{NH}_4)_2\text{C}_2\text{O}_4 \cdot \text{H}_2\text{O}$ , Merck, 99% purity), sodium hydroxide (NaOH, Merck, 99.99% purity) were supplied as initial reagents to synthesize CdO nanostructure. Congo Red (CR),  $\text{C}_{32}\text{H}_{22}\text{N}_6\text{Na}_2\text{O}_6\text{S}_2$ , with molecular weight  $696.66 \text{ g mol}^{-1}$  (Merck) was used as a model dye. Deionized and distilled water were used to prepare all solutions.

### 2.2. Characterization

The powder X-ray diffraction (XRD) measurements were carried out by a JEOL diffractometer with monochromatized  $\text{Cu K}\alpha$  radiation ( $\lambda = 1.5418 \text{ \AA}$ ). Fourier transform infrared (FT-IR) spectra were recorded on a Shimadzu-8400S spectrometer in the range of  $400\text{-}4000 \text{ cm}^{-1}$  using KBr pellets. Scanning electron microscopy (SEM) images were obtained on a Philips (XL-30) with gold coating. Thermogravimetric analysis (TGA) measurement was carried out on a NETZSCH TG 209 F1 Iris apparatus with a heating rate of  $10 \text{ }^\circ\text{C min}^{-1}$  under nitrogen atmosphere. A double-beam UV spectrophotometer (Shimadzu UV-1700) was used for determination of CR concentration in the supernatant solutions before and after adsorption.

### 2.3. Synthesis method

In order to synthesize CdO rhombus-like structure,  $\text{CdCl}_2 \cdot \text{H}_2\text{O}$  and  $(\text{NH}_4)_2\text{C}_2\text{O}_4 \cdot \text{H}_2\text{O}$  as starting materials with a molar ratio of 1:1 were dissolved in 30 mL of the distilled water at alkaline pH. Alkaline conditions were obtained by adding the certain volume of 1.5 M NaOH solution under ultrasonic waves and continuous

stirring for 30 min so that the pH reaches to 11. The resulting solution was transferred into an 80 mL Teflon-lined stainless steel autoclave and performed the hydrothermal reaction at 160 °C for 24 h. The autoclave was cooled down to room temperature. The resulting precursor was filtered, washed with distilled water and ethanol several times to remove the additional ions and finally dried at 70 °C for 24 h in an air oven. The resulting precipitation (precursor) was calcined at 450 °C for 2 h in a furnace. Finally, the obtained compound was characterized.

#### 2.4. Adsorption behavior of CR dye

Adsorption value was determined in the following conditions: 25 mL of CR dye with a known initial concentration (in the range of 5 mg L<sup>-1</sup> to 50 mg L<sup>-1</sup>) was agitated accompanied by 0.01 g of the adsorbent, prepared CdO rhombus microstructure, on a magnetic stirrer at 25 °C for 2 h in the dark to estimate only adsorption performance. Then CR loaded CdO powder was separated with centrifugation at 1800 rpm for 5 min. The concentration of the residual dye was measured by using UV–VIS spectrophotometer at appropriate wavelength corresponding to the maximum absorption of CR (498 nm). The percent removal of dye from the solution was calculated by the following equation:

$$\% \text{ Removal efficiency} = \frac{C_0 - C_i}{C_0} \times 100 \quad (1)$$

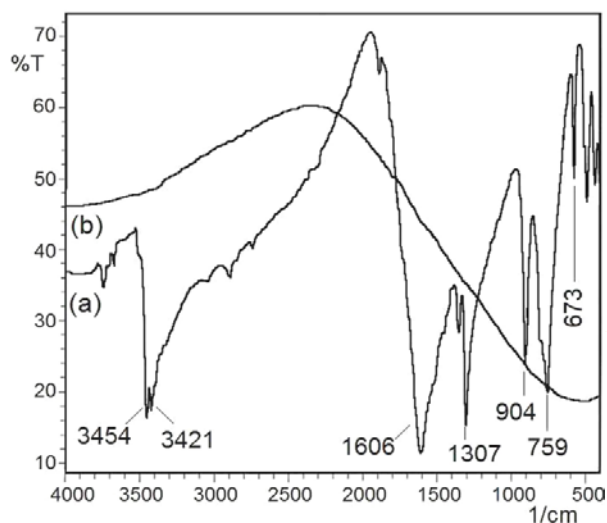
Where  $C_0$  is the initial concentration of dye and  $C_i$  is the final concentration of dye after treatment with CdO rhombus particles. The removal

percentage of CR molecule increased with time due to its adsorption onto adsorbent sites.

### 3. Results and discussion

#### 3.1. Structural study

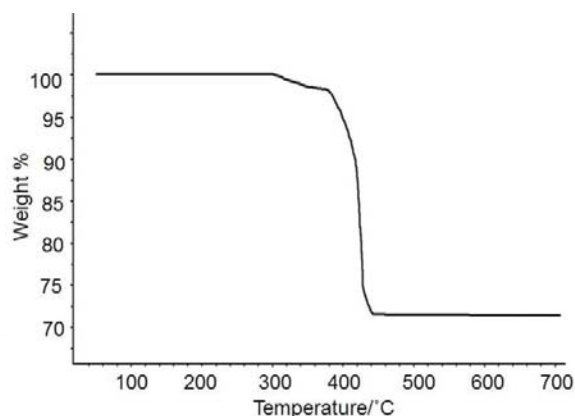
Fig. 1 shows the FT-IR spectra of the obtained precursor from the hydrothermal process (Fig. 1a) and the resulting product of the calcination at 450 °C for 2 h (Fig. 1b). The observed peaks in Fig. 1a are related to the organic groups of the precursor. The absorption bands at 3454 and 3321 cm<sup>-1</sup> are attributed to the N-H antisymmetrical and symmetrical stretching vibrations, respectively, which are in a close agreement with the vibrations of the amine groups. Probably, the overlapping O-H vibration bands of the H<sub>2</sub>O molecules with the vibration bands of the functional groups of NH<sub>2</sub> can lead to broaden these bands. The appeared peaks at 1606 and 1307 cm<sup>-1</sup> are assigned to C=O and C-O stretching vibrations of the carbonyl groups, respectively. Actually, the frequency of the CO vibrations has decreased by the resonance effect. The observed peaks at 904, 759 and 491 cm<sup>-1</sup> can be attributed to the  $\nu(\text{CO})$  and  $\nu(\text{CO}_2)$  [22-24]. Likewise, the appeared peak at 673 cm<sup>-1</sup> can be corresponded to the vibration band of formed Cd-O in the precursor [25]. Due to the heating at 450 °C, the typical peaks of the organic molecules of the precursor were disappeared and no absorption band was observed in the FT-IR spectrum of the obtained product (Fig. 1b). Indeed, the organic section was removed and only the broad band as CdO phase remained.



**Fig. 1.** FT-IR spectra of the precursor as prepared intermediate molecule by hydrothermal reaction (a) and the resultant CdO after calcinating treatment at 450 °C for 2 h (b).

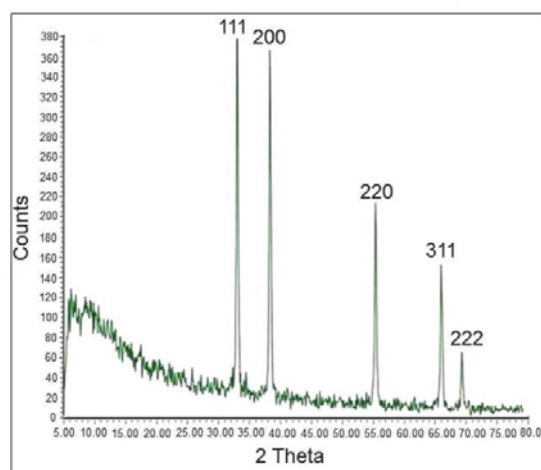
According to the FT-IR data, we can propose the probable reactions for the formation of the intermediate molecule (precursor) and CdO as the resulting product of the hydrothermal reaction.

Fig. 2 illustrates the curve of thermal gravimetric analysis of the precursor. According to this curve, the decay of this compound is performed in a two-step pattern of weight loss. The first weight loss of 1.8 % is observed in the range of temperature between 300 – 380 °C, which can be related to decomposition of adsorbed water molecules. The second weight loss of 29.66% observed in the temperature range between 380-450°C can be attributed to decomposition of the organic sections in the precursor. It was found that the weight loss terminates at 450 °C, so this temperature was determined as the calcination temperature of the intermediate molecules and reaching the CdO phase.



**Fig. 2.** The curve of thermal gravimetric analysis (TGA) of the precursor.

The X-ray diffraction patterns of the products are presented in Fig. 3. Fig 3a shows the XRD pattern of the resultant product after the calcination step. This pattern confirms the formation of CdO phase with a lattice parameter  $a = 4.695 \text{ \AA}$ . The diffraction peaks at  $2\theta$  values of 33.01°, 38.20°, 55.20°, 65.80°, and 69.20° matching with the 111, 200, 220, 311, and 222 planes of cubic CdO (JCPDS- 05-0640) indicated the formation of cadmium oxide phase. No other peaks related to the impurities were detected.



**Fig. 3.** XRD pattern of the obtained CdO nanostructure.

### 3.2. Morphological study

Fig. 4 indicates the SEM images of the obtained CdO nanostructure. The low magnification images of SEM (Figs.4a and 4b) clearly indicate rhombus-like structures with regular facets and the sharp edges between the facets. Meanwhile, high magnification of SEM images shown in Figs. 4c and 4d reveals that the mentioned structure consists of the particles in nanoscale with the average size of 29 nm. It can be found that the special orientation of the nanoparticles can be aggregated into rhombus form. Probably, the coordination mode of the ligand molecules (oxalate ions) to metal ions (cadmium ions) in precursor, before calcining treatment, can lead to this aggregation, which confirms the mentioned FT-IR data and proposed mechanism.

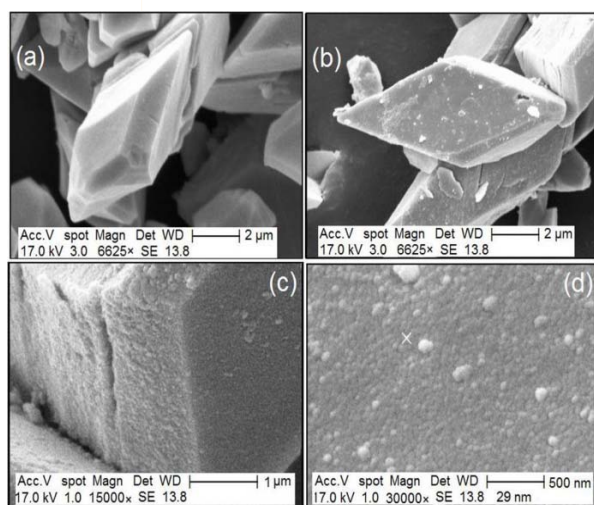


**Fig. 4.** SEM images of CdO rhombus nanostructure obtained from the hydrothermal reaction.

### 3.3. Adsorption investigation

#### 3.3.1. Effect of contact time and pH on removal

The effect of contact time (in the range 0.5-2.5 h) on the adsorption of CR was studied to determine the time taken CdO rhombus-shaped nanostructure to remove  $10 \text{ mgL}^{-1}$  of CR solution at neutral pH. A certain amount of adsorbent, 0.01 g of CdO rhombus particles was added into a 25 mL of CR solution. The decrease in the concentration of CR with time is owing to its adsorption on CdO rhombus structure. The results are shown in Fig 5. According to the mentioned diagram; the maximum removal efficiency of CR dye (97%) occurs about 2h that almost all the CR dye became adsorbed. Likewise the adsorption efficiency of CR was constant after 2.5 h; therefore agitation time of 2h was selected for further studies. Although pH is a significant controlling parameter that intensely influences adsorption efficiency of cationic or anionic dyes onto adsorbent sites, this type of adsorbent presents a well behaviour of adsorption at neutral pH. In fact, adsorption performance at neutral pH is an excellent advantage that few adsorbents show this feature. The most of reports provided by researchers to remove the CR dye are at pH 5 and 6 [26, 27].

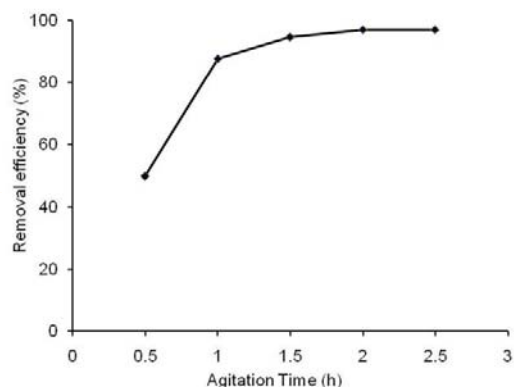


**Fig. 5.** Removal of CR dye in various times. Conditions: 0.01 g CdO rhombus particles, 25 mL of  $10 \text{ mg L}^{-1}$  CR and neutral pH.

### 3.3.2. Effect of amount of CdO rhombus nanostructures

The effect of amount of the adsorbent needed for the maximum recovery of CR dye is shown in Fig. 6. Different quantities of CdO rhombus nanostructures were investigated in the range of 0.005 to 0.015 g. Maximum recovery percentage was specified when 0.01 g of CdO rhombus nanostructures was used in 25 mL solution of CR

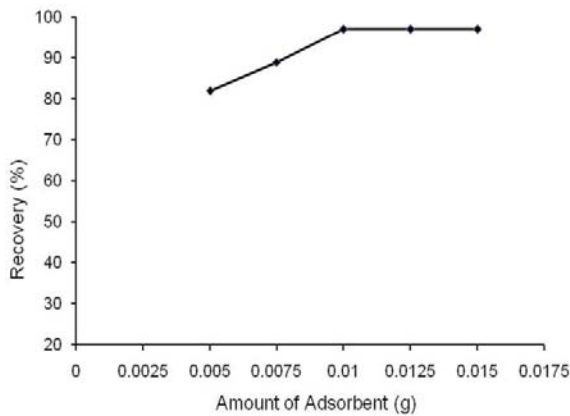


**Fig. 6.** Effect of amount of adsorbent on the recovery of CR removal. Condition: 25 mL of CR dye with  $10 \text{ mg L}^{-1}$  concentration and neutral pH.

dye with  $10 \text{ mg L}^{-1}$  concentration at neutral pH. Therefore further studies were conducted on CR dye at optimum amount of mentioned adsorbent.

### 3.3.3. Adsorption Isotherm

Fig. 7 shows the capacity of CdO rhombus structures to adsorb CR solution studied by measuring the initial and final concentration of CR in the dark for 2 h. It is found that the adsorption of CR molecules increases with the concentration of dye solution and inclines to

reach the saturation point at higher concentrations ( $40$  and  $50 \text{ mg L}^{-1}$ ). Langmuir equation, a famous adsorption isotherm pattern, was applied to examine the relationship between the amount of CR adsorbed onto CdO rhombus particles and its equilibrium concentration in solution. This process was found to obey very well from Langmuir model. Although Langmuir's model does not consider the variation in adsorption energy, it obviously describes the adsorption method. It is based on the physical theory that the maximum adsorption capacity includes of a monolayer adsorption [28]. The general form of Langmuir isotherm equation is as follows:

$$\frac{q_e}{K_L} = \frac{a_L C_e}{1 + K_L C_e} \quad (2)$$

After linearization of the Langmuir isotherm, Eq.3, we obtain:

$$\frac{C_e}{q_e} = C_e \left( \frac{a_L}{K_L} \right) + \left( \frac{1}{K_L} \right) \quad (3)$$

$a_L$  ( $\text{L mg}^{-1}$ ) and  $K_L$  ( $\text{L g}^{-1}$ ) are the Langmuir constants. These constants were calculated from the slope and intercept of the plot of  $C_e/q_e$  vs.  $C_e$  in Fig. 8.  $C_e$  is the equilibrium concentration of the CR in the solution ( $\text{mg L}^{-1}$ ).  $q_e$ , the amount of CR adsorbed ( $\text{mg g}^{-1}$ ) per unit of adsorbent at equilibrium ( $\text{mg g}^{-1}$ ), was calculated by equation as given below:

$$q_e = \frac{V(C_i - C_f)}{m} \quad (4)$$

Where  $C_i$  and  $C_f$  are the initial and final concentrations of CR in  $\text{mg L}^{-1}$ , respectively;  $V$  is

the volume of experimental solution in L, and  $m$  is the weight of CdO rhombus particles in g.

The maximum adsorption capacity ( $\text{mg g}^{-1}$ ) is indicated by  $[Q_m = K_L/a_L]$ . As the  $q_{\text{max}}$  highly depends on the number and structure of adsorption sites, current study aimed at preparing CdO rhombus structures to increase the contact sites and the number of available sites in accord with sharp edges of rhomb structure. As long as there are unoccupied sites, adsorption process will resume with increasing CR concentrations, but as soon as all of the adsorbent sites are filled, an additional increase in concentrations of CR solutions does not increase the amount of CR on adsorbents [29].

The parameters of the Langmuir equation were calculated and given in Table 1. The maximum adsorption capacity ( $q_{\text{max}}$ ) for adsorption of CR onto CdO rhombus structures was found to be  $41.2 \text{ mg g}^{-1}$ . This value is higher than that of other adsorbents such as hollow  $\text{Zn-Fe}_2\text{O}_4$  nanospheres [26], bagasses fly ash [30], chitosan montmorillonite [31] acid activated red mud [32], and Anilinepropylsilica xerogel [27]. However, another study on maghemite nanoparticles has been also reported with  $q_{\text{max}}$  much higher than present work [28].

#### 3.4.4. Mechanism of adsorption

CdO rhombus particles have the surfaces (sharp edges of rhomb) or sites which have been positively charged related to the metal cation of  $\text{Cd}^{2+}$ . As CR dye is an anionic compound, a strong electrostatic interaction between adsorption sites of adsorbent and dye anions leads to remove the CR molecules from solution in the short time.

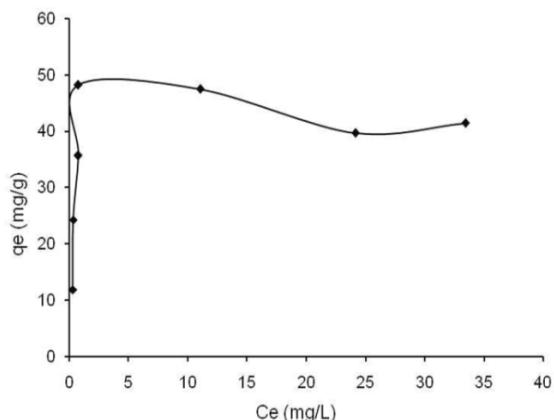


**Fig. 7.** Adsorption isotherm of CR on CdO rhombus particles. Conditions: ambient temperature, neutral pH, 25 mL of CR dye with known initial concentrations (in the range of  $5 \text{ mg L}^{-1}$  to  $50 \text{ mg L}^{-1}$ ) and 0.01 g of adsorbent.

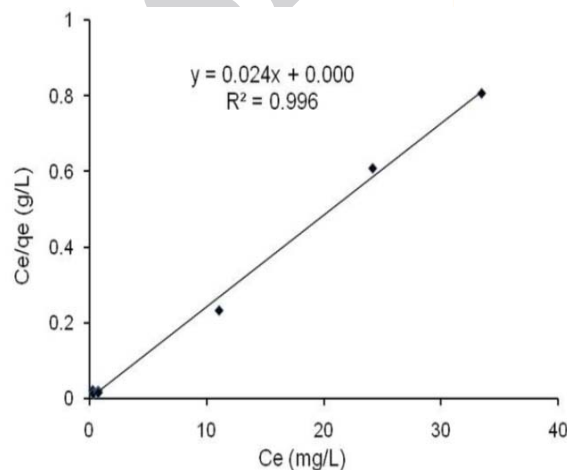


**Fig. 8.** Langmuir plots for the adsorption of Congo Red.

## 4. Conclusion

In a summary, we successfully synthesized the rhombus-shaped structure of CdO by using hydrothermal method and then calcination treatment at  $450 \text{ }^\circ\text{C}$  for 2 h. The SEM images clearly revealed that the rhombus structure consists of uniform nanoparticles with the average size of 29 nm. The present study indicates that the prepared CdO rhombus-like can be considered as an adsorbent with a qualified

efficiency to remove CR dye from aqueous solutions in high concentrations (5–50 ppm) and the maximum adsorption capacity ( $q_{\max}$ ) for it was found to be 41.2 mg g<sup>-1</sup>. Decolorizing efficiencies of the obtained CdO particles was measured about 99%. Accordingly, the prepared sample can be a promising candidate for further studies.

### Acknowledgements

The financial support of this study, by Iran University of Science and Technology and Iranian Nanotechnology Initiative, is gratefully acknowledged.

### References

- [1] A. S. Kalathur, Cathodic electrodeposition of cadmium oxide, zinc oxide and mixed cadmium oxide-zinc oxide thin films M.Sc. Thesis, The University of Texas at Arlington (2005).
- [2] W. Dong, C. Zhu, *Opt. Mater.* 22 (2003) 227-233.
- [3] R. Vinodkumar, K.J. Lethy, P.R. Arunkumar, R.R. Krishnan, N. Venugopalan Pillai, V.P. Mahadevan Pillai, R. Philip, *Mater. Chem. Phys.* 121 (2010) 406-413.
- [4] M.A. Grado-Caffaro, M. Grado-Caffaro, *Phys. Lett. A* 372 (2008) 4858-4860.
- [5] A. Gulino, G. Compagnini, A.A. Scalisi, *Chem. Mater.* 15 (2003) 3332-3336.
- [6] A.A. Ziabari, F.E. Ghodsi, *J. Alloy Compd.* 509 (2011) 8748-8755.
- [7] F. Yakuphanoglu, *Appl. Surf. Sci.* 257 (2010) 1413–1419.
- [8] Z.R. Ranjbar, A. Morsali, *Polyhedron* 30 (2011) 929-934.
- [9] N. Varghese, L.S. Panchakarla, M. Hanapi, A. Govindaraj, C.N.R. Rao, *Mater. Res. Bull.* 42 (2007) 2117-2124.
- [10] T. Ghoshal, S. Kar, S.K. De, *Appl. Surf. Sci.* 255 (2009) 8091-8097.
- [11] S. Ashoka, P. Chithaiah, G.T. Chandrappa, *Mater. Lett.* 64 (2010) 173-176.
- [12] A. Tadjarodi, M. Imani, *Mater. Res. Bull.* 46 (2011) 1949-1954.
- [13] A. Tadjarodi, M. Imani, *Mater. Lett.* 65 (2011) 1025-1027.
- [14] K. Byrappa, T. Adschiri, *Progr. Cryst. Growth Char. Mater.* 53 (2007) 117-166.
- [15] C. Karunakaran, R. Dhanalakshmi, *Cent. Eur. J. Chem.* 7 (2009) 134-137.
- [16] C. Karunakaran, R. Dhanalakshmi, P. Gomathisankar, G. Manikandan, *J. Hazard. Mater.* 176 (2010) 799-806.
- [17] A. Nezamzadeh-Ejhi, Z. Banan, *Desalination* 279 (2011) 146-151.
- [18] H.Y. Zhu, Y.Q. Fu, R. Jiang, J.H. Jiang, L. Xiao, G.M. Zeng, S.L. Zhao, Y. Wang, *Chem. Eng. J.* 173 (2011) 494-502.
- [19] A. Rodríguez, J. García, G. Ovejero, M. Mestanza, *J. Hazard Mater.* 172 (2009) 1311-1320.
- [20] R. Suárez-Parra, I. Hernández-Pérez, M.E. Rincón, S. López-Ayala, M.C. Roldán-Ahumada, *Sol. Energ. Mater. Sol. Cell* 76 (2003) 189-199.
- [21] A. Tor, Y. Cengeloglu, *J. Hazard. Mater.* 138 (2006) 409-415.
- [22] F. F. P. Medeiros, M. F. V. Moura, A. G. P da Silva, C. P. Souza, K. K. P. Gomes, U. U. Gomes, *Braz. J. Chem. Eng.* 23 (2006) 531-538.
- [23] D.L.G.L. Pavia, G.S. Kriz, J.R. Vyvyan, *Introduction to Spectroscopy*, fourth ed., Brooks/Cole Cengage Learning, United State, 2009.



- [24] K. Nakamoto, *Infrared Raman Spectra of Inorganic and Coordination Compounds*, sixth ed., John Wiley & Sons, Inc., Hoboken, New Jersey, 2009.
- [25] S.C. Singh, R.K. Swarnkar, R. Gopal, *AIP Conf. Proceed.* 1147 (2009) 211-215.
- [26] R. Rahimi, H. Kerdari, M. Rabbani, M. Shafiee, *Desalination* 280 (2011) 412–418.
- [27] S. Chatterjee, D. S. Lee, M. W. Lee, S. H. Woo, *Bioresource Technol.* 100 (2009) 2803–2809.
- [28] F. A. Pavan, S. L.P. Dias, E. C. Lima, E. V. Benvenutti, *Dyes Pigments* 76 (2008) 64-69.
- [29] A. Afkhami, R. Moosavi, *J. Hazard. Mater.* 174 (2010) 398–403.
- [30] S. Wang, Z.H. Zhu, *J. Hazard. Mater.* 126 (2005) 91-95.
- [31] L. Wang, A. Wang, *J. Hazard. Mater.* 147 (2007) 979–985.
- [32] A. Tor, Y. Cengeloglu, *J. Hazard. Mater. B* 138 (2006) 409–415.

Archive of SID